

Trans-dominant inhibition of RNA viral replication can slow growth of drug-resistant viruses

Scott Crowder & Karla Kirkegaard

The high error rates of viral RNA-dependent RNA polymerases create heterogeneous viral populations whose disparate RNA genomes affect each other's survival. We systematically screened the poliovirus genome and identified four sets of dominant mutations. Mutated alleles in capsid- and polymerase-coding regions resulted in dominant negative phenotypes, probably due to the proteins' oligomeric properties. We also identified dominant mutations in an RNA element required for priming RNA synthesis (CRE) and in the protein primer (VPg), suggesting that nonproductive priming intermediates are inhibitory. Mutations that inhibit the activity of viral proteinase 2A were dominant, arguing that inhibition of its known intramolecular activity creates a toxic product. Viral products that, when defective, dominantly interfere with growth of nondefective viruses will probably be excellent drug targets because drug-sensitive viruses should be dominant over drug-resistant variants. Accordingly, a virus sensitive to anticapsid compound WIN51711 dominantly inhibited the intracellular growth of a drug-resistant virus. Therefore, dominant inhibitor screening should validate or predict targets for antiviral therapy with reduced risk for drug resistance.

The error-prone replication of RNA viral genomes enables them to evolve resistance to selective agents rapidly and effectively¹. For cytoplasmic positive-strand RNA viruses, including poliovirus, other picornaviruses such as foot-and-mouth disease virus, and more distantly related flaviviruses such as dengue and West Nile viruses, an infection started by a single virus can quickly become heterogeneous, even in the first infected cell. Therefore, a progeny genome containing a new mutation that could confer a selective advantage must replicate and package in the context of an essentially polyploid infection in order to propagate. Are the products of advantageous alleles shared with other, 'nonadvantaged' genomes in the same cell, or is their benefit conferred only to the genome that encodes them, in *cis*? Could nonadvantaged alleles be dominant and therefore mask the growth of genomes that encode, for example, drug-resistant products?

Consistent with the latter possibility, dominant mutations in the capsid-coding regions of poliovirus and other picornaviruses have been reported²⁻⁴. In vesicular stomatitis virus, a negative-strand RNA virus, the phenomenon of 'phenotypic masking' was observed during the selection of viruses resistant to neutralization by monoclonal antibodies⁵. Neutralization-resistant variants were isolated at frequencies far lower than predicted from the measured polymerase error rate. Because capsid proteins function as higher-order oligomers, a plausible explanation of phenotypic masking is that the neutralization-sensitive capsid proteins encoded by the parental genomes mixed with neutralization-resistant proteins encoded by the mutated genomes to form chimeric virions. Assuming that the inclusion of even a few neutralization-sensitive capsid proteins could render a chimeric virion

neutralization-sensitive, the sensitive genomes would be expected to be dominant over the resistant ones, explaining the observed result.

The viral capsid is not the only oligomeric complex formed during viral amplification. For poliovirus, membrane-associated proteins 2B, 2C, 2BC, 3A, 3AB, 3CD proteinase and 3D polymerase (Fig. 1a) and an RNA element required for priming (CRE) all form hetero- or homo-oligomeric complexes⁶. Investigation of the genetic properties of 31 nonviable poliovirus genomes showed that they had markedly different, locus-specific effects on cotransfected wild-type genomes. We suggest that, for poliovirus and other viruses with facile reverse genetics, such a dominant inhibitor screen can identify regions of the genome that, when mutated, lead to the formation of inhibitory complexes. Loci that contain such dominant mutations will identify targets for antiviral compounds that will be relatively resilient to the growth of drug-resistant viruses.

RESULTS

Design and characterization of nonviable mutant polioviruses

To search for dominant mutations in a comprehensive, genome-wide manner, we constructed a series of poliovirus genomes with lethal mutations spanning the coding region (Table 1). The construction of each mutant genome was guided by either a previously described mutation or a strategy to disrupt the structure of the encoded protein. By targeting predicted hydrophobic cores or α -helices, we introduced 23 individual U \rightarrow C mutations into an infectious poliovirus cDNA. We then tested the viability of each mutated viral genome (Table 1). For 20 of the 23 mutations, we detected no virus after a single cycle of growth after RNA transfection, indicating that there was no reversion

Department of Microbiology and Immunology, Stanford University School of Medicine, Stanford, California 94305-5124, USA. Correspondence should be addressed to K.K. (karlak@stanford.edu).

Published online 19 June 2005; doi:10.1038/ng1583

to wild-type virus. The other three mutations gave rise to viable viruses with temperature-sensitive phenotypes, which we characterized further (Supplementary Table 1 online). For both previously published and newly designed mutations, we considered only those mutated genomes that resulted in at least 100,000 times less plaque formation after RNA transfection to be nonviable and used these to screen for dominant negative poliovirus mutations.

Dominant negative mutations in capsid-coding regions

To test the ability of nonviable mutated viral genomes to affect growth of wild-type viruses, we cotransfected HeLa cells with nonviable and wild-type viral RNAs, collected the intracellular virus after a single replicative cycle and titered the resulting wild-type virus stocks. To mimic a scenario in which a drug-resistant genome emerges from a drug-sensitive population, and to optimize cotransfection conditions, we used a tenfold excess of the nonviable genome. We substituted total yeast tRNA for mutant RNA in the positive wild-type control. Under these conditions, transfection of $\sim 2 \times 10^6$ cells with 100 ng of wild-type RNA typically yielded a virus stock of 5×10^4 to 2×10^5 plaque-forming units (PFU) per milliliter.

We tested the effect of a known inhibitor of poliovirus RNA replication, an RNA transcript (R2-PvuII) made *in vitro* from a poliovirus cDNA template cleaved with PvuII (ref. 7), to ensure that our transfection protocol led to cotransfection of the wild-type and potentially inhibitory genomes. When cotransfected with wild-type viral RNA, a tenfold excess of R2-PvuII RNA inhibited wild-type growth (Fig. 1b), as reported previously⁸. The mechanism by which R2-PvuII RNA inhibits wild-type growth is not known, but wild-type growth was inhibited by more than 95%, suggesting that at least 95% of the cells that contained wild-type viral RNA also contained the cotransfected inhibitor RNA.

We used a frameshift control, VP1-M158fs, that contains a mutation in the center of the VP1-coding region and produces a truncated wild-type polyprotein with termination of translation at a stop codon 14 amino acid residues downstream from the frameshift in VP1. Cotransfection of either VP1-M158fs or another lethally mutated RNA, 3A-L24S, had little effect or caused a slight increase in wild-type yield (Fig. 1b).

In contrast, all four genomes that contained lethal mutations in the capsid-coding region, VP2-S1P, VP2-S243P, VP3-L211S and VP1-L118P, reduced wild-type viral growth 90–95% (Fig. 1), similar to R2-PvuII. On average, capsid mutants inhibited wild-type growth by 93%.

Allele-specific inhibition by mutations in the 3D polymerase coding region

Because the poliovirus RNA-dependent RNA polymerase can oligomerize⁹, we tested the dominance of five different nonviable mutations in the polymerase-coding region

(Fig. 2a,b). One mutation, S291P, diminished wild-type viral growth to 1% of that of the control (Fig. 2c), having a larger dominant effect than the R2-PvuII cotransfection control. Two other mutations, F30S and F191S, diminished wild-type growth to 29% and 13% of that of the control, respectively, and were therefore defined as codominant. Other mutations had variable intermediate or helper effects and were defined as recessive. Mapped onto the fully resolved 3D polymerase structure¹⁰, most mutant residues cluster in the hydrophobic core of the fingers domain; 3D-F30S is located at the junction between the 'finger' and 'thumb' domains (Fig. 2b). The variability in observed dominance of 3D polymerase mutations may reflect varying degrees of protein stability or the oligomerization potential of 3D polymerase or its precursors, such as 3CD proteinase.

Dominant mutations of the protein primer 3B and an RNA element

We next assessed the *trans*-dominant effects of mutations of the *cis*-acting replication element (CRE), which templates VPg uridylylation

Table 1 Mutated poliovirus genomes used in the dominance screen

Mutant	Codon change	Rationale	Viability (PFU/ml)
Previously characterized mutated genomes			
VP2-S1P	UCG → CCG	Maturation cleavage ³⁸	<5
VP2-S243P	UCC → CCC	Antibody neutralization ³⁹	<5
VP1-M158fs	NA	Frameshift mutation	<5
VP1-Y302P	TAT → CCT	VP1-2A cleavage site ¹⁹	<5
VP1-T301R	ACA → CGA	VP1-2A cleavage site ¹⁹	<5
2A-C109R	UGU → CGU	Catalytic proteinase ⁴⁰	<5
3B-Y3H	UAC → CAC	Uridylylation site ^{41,42}	<5
3C-C147R	UGU → CGU	Catalytic proteinase cysteine ⁴³	<5
3D-F30S	UUC → UCC	Fingers-thumb interaction ^{44,45}	<5
3D-S291P	UCA → CCA	Inactivating insertion ⁴⁶	<5
CRE-C4465U-U4483C*	None	Nonviable mutant ⁴⁷	<5
CRE-G4462A-U4483C*	None	Nonviable mutant ⁴⁷	<5
Newly designed mutated genomes			
VP2-F260S	UUC → UCC	Hydrophobic	<5
VP3-F118S	UUU → UCU	Hydrophobic	<5
VP3-L211S	CUU → CCU	Hydrophobic	<5
VP1-L118P	UUA → UCA	Hydrophobic & helix	<5
2A-S74P	UCC → CCC	Helix	TS
2A-L98P	CUC → CCC	Hydrophobic	<5
2B-F12S	UUU → UCU	Hydrophobic & helix	<5
2B-F16S	UUU → UCU	Hydrophobic & helix	<5
2C-F28S	UUC → UCC	Hydrophobic & helix	TS
2C-L93P	CUU → CCU	Hydrophobic	<5
2C-F242S	UUU → UCU	Hydrophobic	<5
2C-F328S	UUU → UCU	Hydrophobic & helix	<5
3A-L8S	UUG → UCG	Hydrophobic	<5
3A-L24S	UUG → UCG	Hydrophobic & helix	<5
3A-F83S	UUU → UCU	Hydrophobic	<5
3C-L70P	CUU → CCU	Hydrophobic	<5
3C-L102S	UUG → UCG	Hydrophobic	<5
3D-F34L	UUU → CUU	Hydrophobic	TS
3D-L107P	CUA → CCA	Hydrophobic	<5
3D-F191S	UUU → UCU	Hydrophobic & helix	<5
3D-F246S	UUC → UCC	Hydrophobic & helix	<5
3D-F296S	UUU → UCU	Hydrophobic & helix	<5
3D-Y326H	UAU → CAU	Hydrophobic	<5

*Mutants in the CRE are double mutants because viruses containing either single mutation were viable. CRE mutations alter nucleotides in the 2C coding region but not the translation of 2C. NA, not applicable; TS, temperature-sensitive.

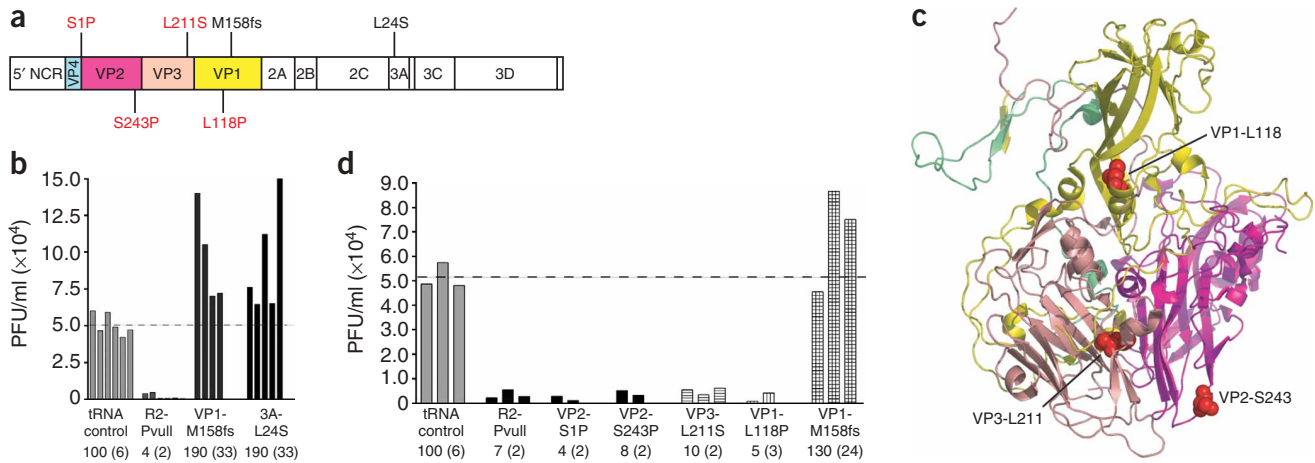


Figure 1 Dominant inhibitor screen for capsid-coding genome regions. **(a)** Schematic of mutated genomes tested as dominant inhibitors of wild-type virus growth. **(b)** Validation of dominant inhibitor screen for R2-PvuII, a known RNA inhibitor of poliovirus growth, and two mutations, a frameshift after wild-type VP1 amino acid 158 (VP1-M158fs) and 3A-L24S, that each provide apparent helper function. Mean values (and s.e.m. in parentheses) from each set of replicate experiments are shown, normalized to the average of the wild-type poliovirus RNA with carrier tRNA control. **(c)** Capsid mutations mapped to the crystal structure of capsid proteins (VP4 in cyan, VP1 in yellow, VP2 in magenta and VP3 in salmon; Protein Data Bank). **(d)** The effect of cotransfecting cells with the indicated RNAs and wild-type RNA on yield of wild-type poliovirus (shown as in **b**).

*in vitro*¹¹, and 3B (the VPg coding region; **Fig. 3a**). Two noncoding double mutations in the CRE, G19A-U40C and C22U-U40C, as well as a mutation of the genome-linked structural protein 3B-Y3H, strongly inhibited growth of wild-type virus (**Fig. 3b**). The degree of inhibition was similar to or greater than that exerted by R2-PvuII, the cotransfection control, or any of the capsid alleles.

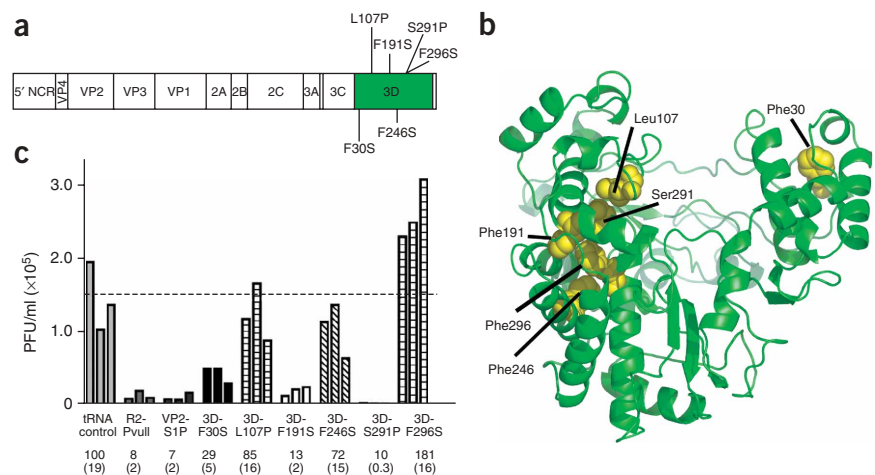
A 'classic' dominant negative mutation is one that disrupts the function of a protein or sequence element but maintains an associative property, such as a protein-protein or protein-RNA interaction¹². For the dominant negative mutations of the CRE, the stem-loop structure is predicted to be maintained (**Fig. 3a**)¹³. But the introduction of eight noncoding mutations into the CRE is predicted to disrupt the stem-loop structure completely¹⁴. This predicted loss-of-function CRE mutation did not inhibit wild-type growth (**Fig. 3c**). Therefore, dominant inhibition by genomes carrying mutations of CRE is allele-specific, presumably requiring an intact RNA stem-loop structure to form an inhibitory complex. Such a complex would probably involve 3CD, a precursor known to bind RNA sequences in the 5' noncoding region as well as the CRE^{13,15}.

Allele-specific dominance in 2A proteinase-coding region

Two different mutations in the 2A proteinase coding region (2A-L98P and 2A-C109R; **Fig. 4a,b**) gave rise to a dominant phenotype (**Fig. 4c**) that correlated with proteinase deficiency. *In vitro* translation^{16,17} of these mutated genomes resulted in the unusual accumulation of uncleaved VP1-2A precursors (**Fig. 4d**). Further experiments in which only the VP1-2A region was expressed *in vitro* recapitulated this proteinase-deficient phenotype (data not shown).

The dominance of proteinase-deficient 2A alleles was somewhat unexpected, because 2A proteinase is a monomeric enzyme with several viral and cellular substrates. Its activity at the VP1-2A cleavage site is thought to be exclusively intramolecular, because cleavage is unaffected by antibodies to 2A and occurs with increased rate and altered specificity relative to intermolecular 2A proteinase cleavages^{18,19}. A 2A protein that lacked enzymatic activity could therefore yield an uncleaved VP1-2A fusion molecule that functions as a dominant negative inhibitor of wild-type growth, like a mutant 2A cleavage site to allow accumulation of the uncleaved VP1-2A

Figure 2 Effect of mutations in 3D polymerase on the yield of wild-type virus during cotransfection. **(a)** Schematic diagram of poliovirus genomes indicating locations of coding regions for mutated 3D polymerase alleles. **(b)** Mutations mapped to the three-dimensional structure of 3D polymerase¹⁰. **(c)** Parallel cotransfection experiments with wild-type RNA and viral genomes containing several different mutations in the coding region for 3D polymerase (shown as in **Fig. 1**).



product from mutated genomes and studied its effect on the growth of coinfecting wild-type virus. Two introduced mutations reported to abrogate 2A-mediated cleavage of the VP1-2A cleavage site, VP1-Y302P and VP1-T301R¹⁹, were also dominant (Fig. 4e). Therefore, uncleaved VP1-2A is toxic to coinfecting wild-type virus, and its accumulation in cells infected with 2A proteinase-deficient mutant viruses is a likely mechanism for their genetic dominance.

Translation and RNA replication requirements for dominance

Genomes that contain capsid mutations are usually competent for RNA replication; therefore, the observed dominance of such genomes may be augmented by the replication of the mutated genomes, resulting in the production of high concentrations of mutant capsid proteins. To determine whether mutated capsid alleles require RNA replication to exert their dominant effects, we introduced a second mutation, Δ GUA₃, into one of the dominant mutated genomes, VP2-S243P. The Δ GUA₃ mutation, a deletion of nucleotides 7418–7422 in the 3' non-coding region (Fig. 5a), severely diminishes negative-strand RNA synthesis²⁰. The doubly mutated genome VP2-S243P- Δ GUA₃ did not inhibit wild-type virus growth (Fig. 5b). Therefore, the dominance of the VP2-S243P allele, and probably the other capsid alleles, requires replication of the mutated RNA genome, presumably leading to increased accumulation of mutant capsid proteins.

As with capsid alleles, 3D polymerase functions can be rescued *in trans* by polymerase molecules encoded by the cotransfected wild-type genomes, enabling genomes with mutated 3D polymerase alleles to replicate at some level^{8,21,22}. We assessed whether the

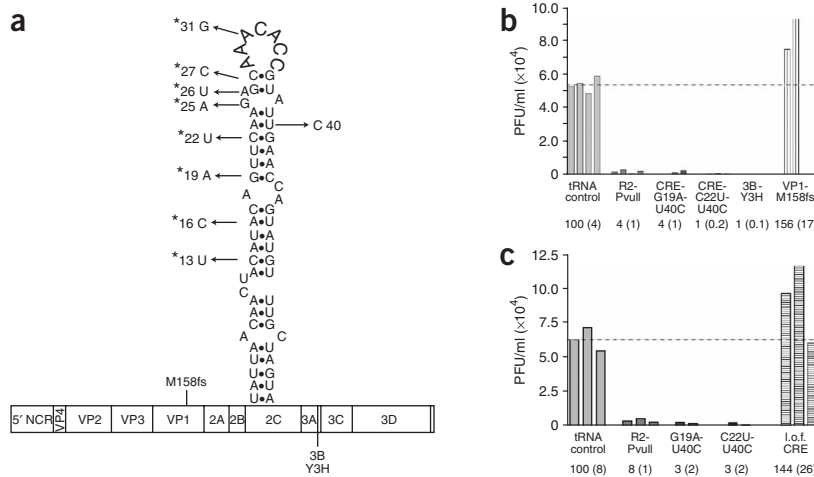


Figure 3 Dominant inhibitor screen in the CRE- and 3B-coding regions. **(a)** A schematic diagram of the predicted secondary structure of wild-type CRE, which resides in the coding region of 2C, indicating mutations G19A, C22U and U40C used in the dominance screen. CRE mutants G19A-U40C and C22U-U40C correspond to genomic nucleotide positions 4462 and 4483 and 4465 and 4483, respectively, and are noncoding⁴⁷. 3B encodes the protein primer, VPg, to which uridyil residues are attached at Tyr3. Asterisks (*) denote mutated nucleotides, which do not alter the translation of 2C, to form the putative loss of function (I.o.f.) CRE¹⁴ used in **c**. **(b)** Cotransfection experiments were done by mixing wild-type and mutated genomes containing the indicated mutated alleles. **(c)** Specificity of mutated CRE alleles. Cotransfections of wild-type and mutated genomes containing the specified CRE alleles were done as described for **Figure 1**.

dominance of the 3D-S291P allele depended on the ability of the genome to replicate by introducing the Δ GUA₃ deletion. The 3D-S291P genome was no longer dominant when its RNA replication was inhibited (Fig. 5c). Like the inhibitory effects of mutant capsid proteins, the high concentration of defective polymerases provided by a replicating genome is needed to inhibit the growth of coinfecting wildtype virus.

To test whether the observed dominance of the 3B-Y3H mutation required RNA replication to exert dominance, we introduced the Δ GUA₃ mutation into this genome. Like dominant capsid

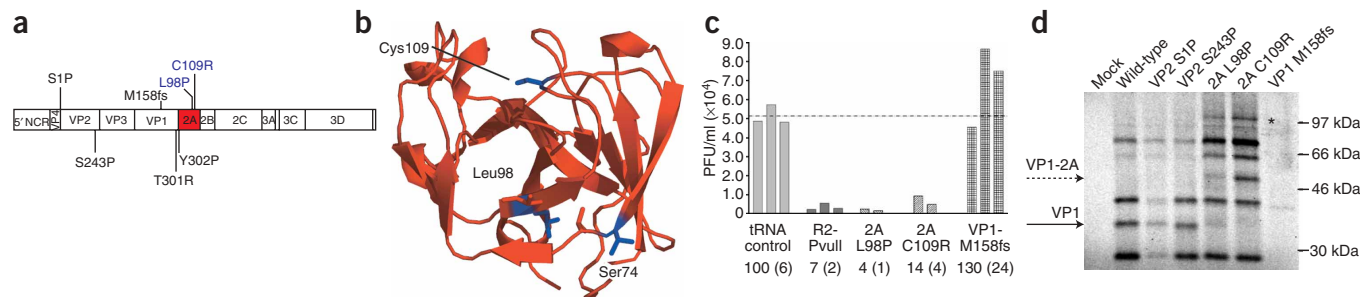


Figure 4 Dominant inhibitor screen for 2A proteinase and VP1-2A cleavage site mutations. **(a)** Schematic diagram of poliovirus genomes indicating relative locations of coding regions for 2A and VP1 and the 2A proteinase and VP1-2A cleavage site mutations used in the dominant inhibitor screen. **(b)** 2A proteinase amino acid residues targeted to generate nonviable mutations used in the dominance inhibitor screen and superinfection assay are mapped onto the crystal structure of 2A proteinase from human rhinovirus 2, a closely related homolog of poliovirus 2A proteinase⁴⁸. **(c)** Cotransfections were done as described for **Figure 1**, and the resulting wild-type virus yields of replicate experiments are shown. Normalization of these values as a percentage of the wild-type RNA with tRNA carrier control is shown (with s.e.m. in parentheses). **(d)** HeLa cytoplasmic lysates were programmed with the indicated poliovirus RNAs and labeled using ³⁵S-methionine, immunoprecipitated with a monoclonal antibody to VP1 and separated on a 10% SDS-PAGE gel. VP1 and VP1-2A mobilities are marked. The asterisk (*) denotes a higher-molecular-weight species abundant in 2A-L98P and 2A-C109R reactions. **(e)** Testing for dominance of genomes with mutated VP1-2A sites was done as described for **Figure 1**.

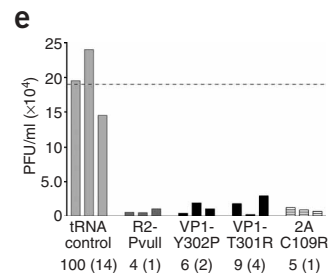
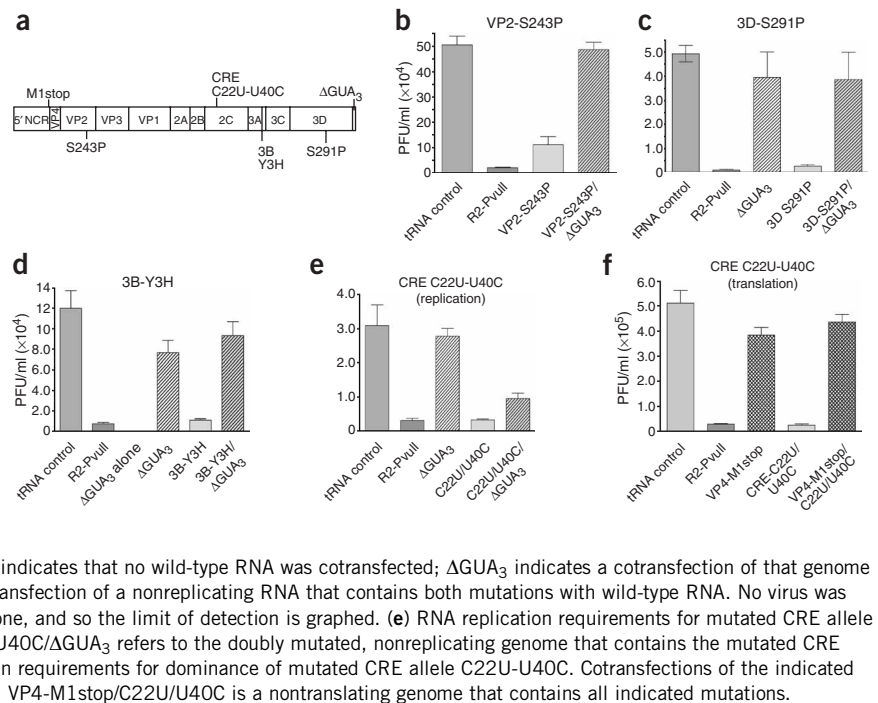


Figure 5 RNA replication or translation requirements for dominance of mutated poliovirus alleles. **(a)** Schematic of mutations mapped to the poliovirus genome assayed for dominance requirements. Δ GUA₃ lacks nucleotides 7418–7422 (GUAAA); RNAs that contain this 3' noncoding region deletion are deficient for negative strand synthesis³⁶. The VP4-M1stop mutation changes the initial methionine of VP4 to a UAG stop codon. **(b)** Test of replication requirement for dominance of the VP2-S243P genome. Cotransfections were done in triplicate; values shown are mean \pm s.e.m. of replicate cotransfections. **(c)** RNA replication requirements for 3D S291P. A mutated genome containing both the 3D-S291P and Δ GUA₃ deletion was cotransfected with wild-type RNA and graphed as in **b**. The cotransfection of wild-type and mutated genomes containing only the Δ GUA₃ deletion is shown as a control. **(d)** RNA replication requirements for a mutation of the RNA replication protein primer 3B-Y3H. Cotransfections were done and graphed as in **b**. Δ GUA₃ alone indicates that no wild-type RNA was cotransfected; Δ GUA₃ indicates a cotransfection of that genome with wild-type RNA. 3B Y3H/ Δ GUA₃ indicates the cotransfection of a nonreplicating RNA that contains both mutations with wild-type RNA. No virus was detected at the highest dilution of the Δ GUA₃ virus alone, and so the limit of detection is graphed. **(e)** RNA replication requirements for mutated CRE allele dominance. Cotransfections were done as in **b**. C22U/U40C/ Δ GUA₃ refers to the doubly mutated, nonreplicating genome that contains the mutated CRE allele and a 3' noncoding region deletion. **(f)** Translation requirements for dominance of mutated CRE allele C22U-U40C. Cotransfections of the indicated genomes containing mutated alleles are shown as in **b**. VP4-M1stop/C22U/U40C is a nontranslating genome that contains all indicated mutations.



and polymerase alleles, the 3B-Y3H allele required replication of its RNA genome to exert dominant negative effects on wild-type growth (Fig. 5d).

When we did the same experiment with dominant negative CRE allele C22U-U40C, however, the triple mutant C22U-U40C- Δ GUA₃ was still inhibitory, suggesting that the mutant CRE structure was toxic at lower concentrations than the defective capsid, polymerase or VPg proteins (Fig. 5e). That such a dominant negative effect could occur without RNA replication is not without precedent; our dominant negative control for cotransfection, R2-PvuII, lacks a 3' noncoding region and also presumably lacks the ability to replicate. To determine whether the CRE RNA alone was the inhibitory moiety, we determined whether a nontranslatable CRE C22U-U40C genome was dominant. We mutated the initial methionine of the poliovirus polyprotein to an amber stop codon (VP4-M1stop) and introduced it into a genome containing the C22U-U40C CRE mutation. The dominant negative phenotype of the C22U-U40C CRE mutation was eliminated when normal translation of the genome was blocked (Fig. 5f). Therefore, it is not the CRE RNA itself, but some complex formed upon translation of viral proteins, that inhibits the growth of other viruses in the same cell. For productive RNA replication

complexes to form on any given poliovirus RNA, translation *in cis* is required⁸. This seems to be the case for the inhibitory complex formed on the mutant CRE also.

Effects in other nonstructural protein-coding regions

The effect of mutations in the 2B-, 2C-, 3A- and 3C-coding regions on cotransfected wild-type viral genomes is shown in **Supplementary Table 2** online. Of the three membrane-associated proteins 2B, 2C and 3A, mutations in 2B were most consistently dominant, although their suppression of wild-type growth was not as pronounced as that of the R2-PvuII control. Partially dominant mutations in the 2B coding region have been reported previously²³. Unlike mutations in 2A proteinase (Fig. 4), mutations in 3C proteinase either were recessive or gave rise to viral genomes that provided a helper function (**Supplementary Table 2** online).

Superinfections of temperature-sensitive and wild-type virus

To test whether the locus- and allele-specific dominance of cotransfected genomes could be observed with viable viruses, we monitored the ability of temperature-sensitive viruses (Fig. 6a) to inhibit the growth of wild-type virus. First, we infected cells with temperature-

Figure 6 Superinfections of wild-type and temperature-sensitive polioviruses. HeLa cells were infected with the temperature-sensitive poliovirus indicated and RNA synthesis was blocked. After mutant proteins were allowed to accumulate, wild-type poliovirus was added to HeLa cells as indicated, and the block to RNA synthesis was released. Viral titers after a single cycle of infection are shown above for two separate experiments at the restrictive temperature. **(a)** Schematic of temperature-sensitive alleles used in superinfections. **(b)** Yield of wild-type virus after superinfection of cells that had accumulated proteins from temperature-sensitive mutant viruses 2A-S74P or 2C-F28S (**Supplementary Table 1** online). **(c)** Yield of wild-type virus after superinfection of cells that had accumulated proteins from temperature-sensitive mutant viruses VP2-R76Q (ref. 24), 3D-F34L (**Supplementary Table 1** online) or 3D-T367I (ref. 25).

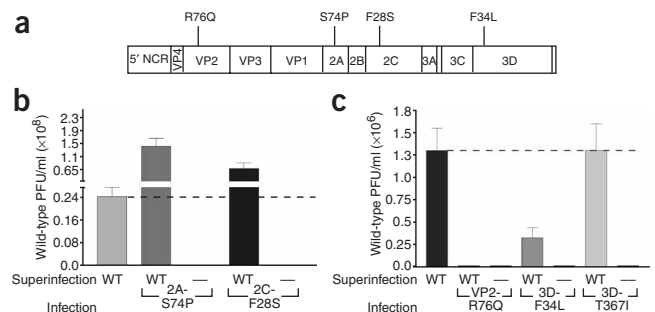
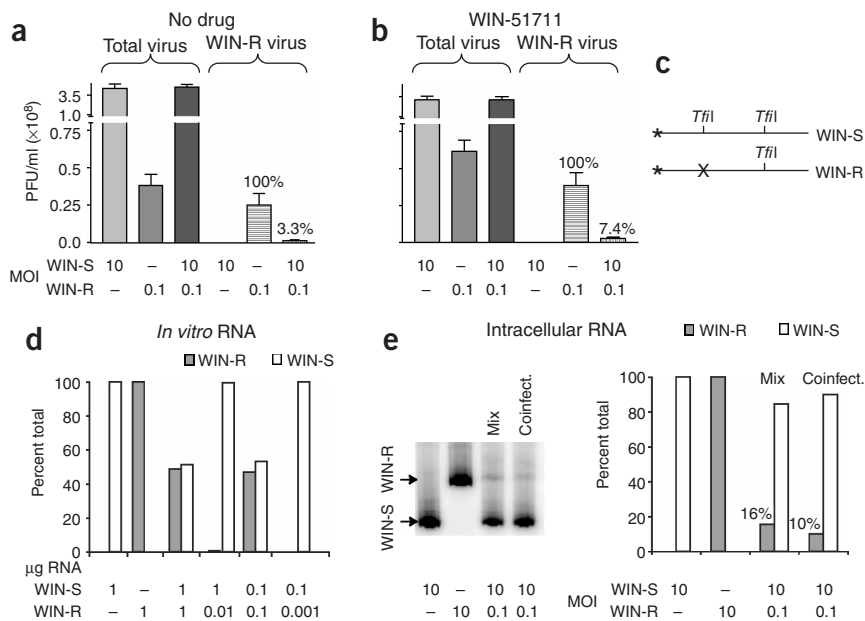


Figure 7 Coinfections of drug-sensitive and drug-resistant viruses. Viral infections were done using either the poliovirus type 3 isolate Fox strain (WIN-S) or a WIN-51711-resistant derivative of the Sabin-3 strain containing a point mutation, VP1-I192F (WIN-R). Infections were done singly or as coinfections, for a single round of virus growth at the indicated MOIs. After virus adsorption, virus growth continued in the absence (a) or presence (b) of 2 $\mu\text{g ml}^{-1}$ of WIN-51711.

To measure total virus, viral titers were determined in the absence of drug; WIN-R virus was measured by adding drug to virus stock dilutions and agar overlays. Percentages refer to the relative amounts of WIN-R virus when WIN-R virus from a single infection is defined as 100%, with standard error measurements indicated by error bars. (c) Schematic of RT-PCR strategy used to measure ratio of WIN-S to WIN-R intracellular RNA. Total intracellular RNA was collected after viral infection of HeLa cells, subjected to RT-PCR using primers common to both WIN-S and WIN-R RNAs and digested with a restriction enzyme, *TfiI*, to quantify the relative abundance of each RNA species. The asterisk (*) denotes the radioactively labeled forward primer; the

differential mobility of the restriction-digested, radioactively labeled RT-PCR product was used to distinguish WIN-R and WIN-S species. (d) Standard curve of *in vitro*-transcribed WIN-R and WIN-S RNA. The indicated RNAs were produced from linearized cDNA templates *in vitro* and added to each RT-PCR reaction. The percentages of total RT-PCR product that migrated as either WIN-S (open bars) or WIN-R (filled bars) are shown for each reaction. The relative intensity of each product was quantified using a phosphorimaging plate and ImageQuant software. (e) Quantification of viral intracellular RNA from infected cells. RT-PCR reactions were done using intracellular RNA collected from the infections indicated in a. Mix refers to a mixing of intracellular RNAs collected from separate single infections of WIN-R and WIN-S viruses; coinfection (coinfect.) refers to the intracellular RNA collected from a coinfection of WIN-R and WIN-S viruses. The relative mobilities of WIN-R and WIN-S digested products are shown. The indicated bands were quantified using a phosphorimaging plate and ImageQuant software. The percentages of total signal for WIN-S or WIN-R are indicated.



sensitive mutant viruses in the presence of an RNA replication inhibitor, guanidine hydrochloride, to allow the mutant viral proteins to accumulate to similar concentrations. Later, we removed guanidine, added wild-type virus and allowed for a single cycle of viral growth at a semipermissive temperature. We then titered the resulting virus stocks at a nonpermissive temperature to quantify the yield of wild-type virus. Viruses with mutations in the 2A proteinase-coding (S74P; Fig. 4b) and 2C NTPase-coding (F28S) regions did not hinder wild-type growth (Fig. 6b), but a virus with a mutation in the capsid-coding region²⁴ (VP2-R76Q) reduced wild-type virus growth by more than 99% (Fig. 6c). We tested the ability of two viruses with different mutations in the coding region for the viral RNA-dependent RNA polymerase, 3D-F34L (Supplementary Table 1 online) and 3D-T367I (ref. 25), to hinder wild-type growth. Virus 3D-T367I was not inhibitory, but virus 3D-F34L inhibited wild-type virus growth by 75%, showing that dominance of mutant viruses, like that of mutated nonviable genomes, was allele- and locus-specific and could be exerted during infections.

Drug-sensitive virus can inhibit drug-resistant virus

The *trans*-acting, highly oligomeric nature of capsid proteins and the observed dominance of capsid mutations suggested that a virus that is resistant to a drug targeting a capsid protein might inhibit a virus that is sensitive to such a drug. Disoxaril (WIN-51711) binds to the 'canyon' residues of poliovirus virions and, by stabilizing the virion structure, prevents the uncoating of the viral genome after cell entry^{26,27}. We introduced a mutation known to confer WIN resistance, VP1-I192F, into a cDNA encoding Sabin-3, the poliovirus serotype most susceptible to WIN-51711 (Fig. 7a,b)²⁸.

To mimic the situation in which a drug-resistant virus appears in a cell infected with wild-type, drug-sensitive virus, we coinfecting cells with wild-type and WIN-resistant polioviruses at a high multiplicity of infection (MOI) for the wild-type virus and a much lower MOI for the drug-resistant virus. The output of WIN-resistant virus was greatly reduced in the presence of drug-sensitive virus, to 3–7% of the yield from a single infection (Fig. 7a,b). Single-cycle coinfections in the absence or presence of the selective agent had similar effects. We hypothesize that the observed dominance of the drug-sensitive genomes was due to chimeric capsid formation, which rendered WIN-resistant genomes susceptible to the drug, being partially encapsidated by WIN-sensitive capsid proteins. Alternatively, RNA replication of the WIN-resistant virus might have been reduced by an unknown mechanism in the coinfection. To test this possibility explicitly, we subjected RNA preparations from all the infections (Fig. 7a) to RT-PCR. We used differential digestion with a restriction enzyme to determine the proportion of WIN-resistant genomes in each preparation (Fig. 7c). Wild-type and mutated genomes could be amplified from mixed populations (Fig. 7d). Similar amounts of WIN-resistant viral RNA were present in the RNA preparations of singly infected and coinfecting cells (Fig. 7e). These results suggest that the reduction in WIN-resistant virus during coinfection was not due to a decrease in RNA replication but to the formation of chimeric capsids that rendered the drug-resistant genome drug-sensitive.

DISCUSSION

We carried out a genomic screen with poliovirus, a positive-strand RNA virus, to identify viral proteins that, when made nonfunctional by mutation, would dominantly interfere with the growth of

cotransfected wild-type viruses. These proteins should be ideal drug targets if the defects of the dominant alleles can be phenocopied by the antiviral compounds. We tested 31 different genomes, each of which contained a lethal mutation. We observed four classes of dominant mutations (**Supplementary Table 3** online). First, as expected, capsid mutations were dominant, presumably because nonfunctional mutant capsid proteins coassemble with wild-type capsid proteins and render the resulting capsid nonfunctional. Second, two of seven mutations in the poliovirus polymerase coding region were dominant. Poliovirus polymerase oligomerizes⁹; therefore, the mechanism of dominance may be similar to that of the capsid alleles. Third, mutations in the CRE, which is required for generation of the protein primer for poliovirus RNA synthesis, were dominant. Finally, mutations that rendered the 2A proteinase of poliovirus inactive (L98P and C109R; **Fig. 4**) were dominant and profoundly inhibitory. The cleavage between VP1- and 2A-coding regions in the viral polyprotein is made by 2A proteinase and reported to be intramolecular¹⁸; it would therefore be refractive to scission in a mutant proteinase even in the presence of mature, wild-type 2A proteinase encoded by coinfecting genomes. We hypothesize that uncleaved VP1-2A protein encoded by the mutated genomes inhibits coinfecting genomes in the same way that mutant capsid protein does: by coassembling with wild-type capsid proteins and poisoning their function. To test this hypothesis, we determined the effects of directly mutating the VP1-2A cleavage site. Such mutations were also dominant.

A direct prediction is that, for a dominant protein target, viruses sensitive to an inhibitor should block growth of drug-resistant viruses. We tested this idea using disoxaril (WIN-51711), which binds to picornaviral capsids²⁹. We found that the presence of WIN-sensitive viruses reduced the yield of WIN-resistant virus, but not WIN-resistant RNA, by 95% (**Fig. 7**).

All these experiments were done within a single round of virus growth to aid in quantifying the dominant effects while avoiding the nonlinear complications introduced by multiple rounds of virus growth. Viral infection of an organism is not constrained to a single round of infection, although any viral genome must be released from the cell in which it first appears in order to propagate. Anecdotal evidence supports a relatively low rate of drug resistance to WIN-51711; this compound was used to treat mice infected with a persistent enterovirus infection over a prolonged period of time without the appearance of drug-resistant isolates³⁰. But viruses resistant to a related compound, pleconaril, could be isolated in tissue culture at a low MOI, a condition in which pre-existing pleconaril-resistant viruses would form plaques without interference from drug-sensitive viruses³¹.

The dominant inhibitor screen described here should aid in identifying good targets for antiviral drug development. If antiviral compounds were designed to phenocopy the deleterious effects of *trans*-dominant mutations, we predict that the drug-sensitive genomes would inhibit the growth of the drug-resistant genomes that would inevitably arise. On the basis of our analysis of poliovirus, we suggest that antiviral compounds that target capsid proteins or specific polymerase domains might result in selection pressure against drug-resistant genomes. For picornaviruses, molecules that phenocopy the effects of mutated CRE and 3B alleles can allow the accumulation of products that are toxic to all genomes in a cell, regardless of genotype.

Perhaps the most practical and generally applicable result presented here is the finding that proteinase-deficient mutations in the poliovirus 2A coding region are dominant. All positive-strand RNA viruses use, to some extent, a polyprotein strategy, in which limited digestion products are excised from larger precursors by viral and, in some cases, cellular proteases. The 1:1 stoichiometry of the viral proteinases

and their targets suggests that some of these cleavages may be preferentially or, in some cases, exclusively intramolecular, as has been documented for poliovirus 2A proteinase¹⁸ and the NS2/3 proteinase of dengue virus³². We predict that the growth of viruses resistant to compounds targeted against such intramolecularly cleaving proteases will be suppressed by the genetic dominance of the inhibitor-sensitive genomes.

METHODS

Design and characterization of mutant genomes used for dominant inhibitor screen. To create nonviable mutated poliovirus genomes, we introduced previously characterized lethal mutations or mutations that were designed to destabilize the structure of the encoded viral protein product using two strategies. The first strategy was to disrupt the hydrophobic core of the encoded protein by reducing the size of an amino acid side chain predicted to be inaccessible to solvent or by changing it to proline. The second strategy was to disrupt predicted α -helices by altering leucine and serine residues predicted to reside in α -helices to proline. We used a computer algorithm, PredictProtein³³, to predict the likely solvent accessibility and α -helicity of each amino acid position within the poliovirus type 1 (Mahoney) polyprotein in its native, folded state. We altered single amino acids presumed to be in the hydrophobic protein core (*i.e.*, having a PredictProtein score >5) by introducing a single U→C transition into the viral genomes using PCR-mediated site-directed mutagenesis³⁴. We used the PredictProtein method instead of relying on known three-dimensional structures to simulate the knowledge base of other, less well-characterized, positive-strand RNA viruses.

We tested the viability of each mutated genome by transfecting 60-mm plates of subconfluent S3 HeLa monolayers with 1 μ g of *in vitro*-transcribed mutant RNA using DEAE-dextran. We collected viral stocks after a single replicative cycle (10 h at 32.5 °C) by pelleting the cells at 200g, washing them and lysing them by freeze-thaw in 1 ml of phosphate buffered saline with 0.1% CaCl₂ and MgCl₂ (PBS+). We then titered stocks as previously described³⁵. Mutated genomes that produced no detectable plaques in this assay were defined as nonviable; 1 μ g of wild-type RNA typically yielded between 4×10^5 and 1×10^6 PFU under these conditions. The results of the engineered and previously characterized mutations are described in **Table 1** and **Supplementary Table 1** online. Reversion of mutant genomes to produce wild-type virus was not detected using DEAE-dextran transfections.

RNA transcription and cotransfections. We linearized plasmids containing the poliovirus 1 genome (pGEM-PV1) under the control of a T7 promoter by digesting them with *EcoRI* (New England Biolabs), purified them by agarose gel electrophoresis and used them as a template for transcription using the Ribomax (Promega) T7 transcription kit in accordance with the manufacturer's standard protocol. We created a control RNA, R2-PvuII, from pGEM-PV1 cDNA that lacks capsid encoding nucleotides 1175–2956 and linearized it with *PvuII*, which cleaves in the coding region of 3D polymerase. We extracted all transcription reactions twice with acid phenol-chloroform (5:1, pH 4.5, Ambion) to remove protein and template DNA and precipitated it with a half volume of 7.5 M ammonium acetate and 2.5 volumes of ethanol. We then resuspended precipitated pellets of RNA in water, applied them to a P30 size exclusion column (Biorad) to remove unincorporated nucleotides and collected the eluate in accordance with the manufacturer's protocol. We verified the integrity of transcribed RNA by denaturing formaldehyde agarose gel electrophoresis (data not shown) and determined the concentration by measuring absorbance at 260 nm. We then reprecipitated the preparations, divided them into aliquots and stored them at –80 °C. We carried out transcription reactions in the presence of α ³²P-UTP to verify that RNA amounts measured by absorbance at 260 nm represented RNA transcripts and not unincorporated nucleotides (data not shown).

We tested the effect of each mutated genome on the growth of wild-type virus by cotransfecting 60-mm plates of subconfluent S3 HeLa monolayers with 1 μ g of *in vitro*-transcribed mutant RNA and 100 ng of wild-type poliovirus RNA using DEAE-dextran (average molecular weight = 500,000; Sigma) as described previously⁸. After incubating them for 10 h at 32.5 °C, we collected cells, produced virus stocks and carried out plaque assays as described³⁵.

In vitro translation of poliovirus RNAs and immunoprecipitation of translation reactions with antibody to VP1. We transcribed poliovirus RNAs as for transfections. We prepared HeLa S10 extracts as previously described³⁶ and programmed a 25- μ l reaction with 5 μ g of RNA, 50% HeLa extract, 1 μ l of ³⁵S-Met Express label (NEN), 0.5 μ l of RNasin (Promega) and 0.5 μ l of 1 mM solutions of each amino acid except methionine. We incubated each reaction for 2 h at 30 °C and stopped them by adding 2 \times lysis buffer (2% Triton X-100 prepared in TBS: 10 mM Tris-Cl (pH 8.0), 140 mM NaCl and 0.025% NaN₃). We then centrifuged each reaction at 10,000g for 30 min at 4 °C. To clear the supernatant, we added 0.05 volumes of a 50% slurry of protein-G sepharose beads (Gibco-BRL), incubated it at room temperature for 2 h and pelleted it by centrifuging for 1 min at 200g. We transferred the supernatant to a new tube precoated with lysis buffer that contained 200 μ l of dilution buffer (0.1% Triton X-100 prepared in TBS). We added monoclonal mouse antibody to VP1 (3 μ g; Chemicon) to each reaction and incubated them for 1.5 h at 4 °C. We pelleted the beads at 200g and washed them twice with dilution buffer, once with TBS and once with 50 mM Tris-Cl (pH 6.8). We then separated protein in the samples on a 10% polyacrylamide gel by SDS-PAGE analysis.

Superinfections. We used temperature-sensitive viruses that were either previously described²⁴ or generated during the screening of nonviable poliovirus type 1 (Mahoney) mutants (**Supplementary Table 1** online). We infected HeLa cell monolayers at an MOI of 100 PFU per cell with each temperature-sensitive virus at a semipermissive temperature of 37 °C in PBS+. After virus adsorption (30 min), we added serum-supplemented Dulbecco's modified Eagle medium with 2 mM guanidine hydrochloride to block viral RNA synthesis. We removed the medium 2 h after infection and superinfected cells with wild-type virus at an MOI of 0.5 PFU per cell. We continued to incubate them at 37 °C for 4 h in the absence of guanidine and then collected cells and made virus stocks as described above. We determined virus titers at 39 °C.

Coinfections of WIN-sensitive and WIN-resistant viruses. We engineered WIN-resistant Sabin 3 virus by introducing a mutation, VP1-I192F, into a cDNA encoding the attenuated Sabin type 3 poliovirus (a gift from A. Macadam, Department of Virology, National Institute for Biological Standards and Control, UK). We carried out infections and coinfections of HeLa cell monolayers at the indicated MOIs for 30 min at 37 °C. We added serum-supplemented Dulbecco's modified Eagle medium (10%) with or without 2 μ g ml⁻¹ final concentration of WIN-51711 (a gift of A. Mosser, University of Wisconsin, Madison, Wisconsin, USA) to the cells and incubated them at 37 °C for 6 h. We then collected cells and titered virus stocks by plaque assay in the absence and presence of 2 μ g ml⁻¹ of WIN-51711 in the agar overlay.

RT-PCR analysis of WIN-R and wild-type RNA. We carried out coinfections and single infections of wild-type and WIN-resistant viruses as described above in the absence of WIN-51711. We collected cells 5 h after infection and processed them by adding 1 ml of Trizol (Invitrogen) to each plate and incubating them for 5 min at room temperature. We extracted the solution with 0.2 ml of chloroform and collected the supernatants. At this time, we created 'mix' samples by combining equal volumes of supernatants derived from single infections (**Fig. 7e**). We collected nucleic acids by adding isopropanol (70%), pelleting by centrifugation, washing with 70% ethanol and repelleting and resuspended the pellets in 50 μ l of 10 mM HEPES-KOH buffer (pH 7.5).

Each reverse transcriptase reaction contained 5 μ l of RNA sample in a final volume of 10 μ l using AMV-RT High Concentration (Promega) as recommended by the manufacturer. PCR reactions (50 μ l total volume) were composed of 5 μ l of a reverse transcriptase reaction and were carried out as previously described³⁷. Reactions were cycled 35 times (94 °C, 1 min; 54 °C, 1 min; 72 °C, 1 min). We used primers that amplified nucleotides 2967–3241 of the type 3 genome. Two *TfiI* restriction sites (at nucleotides 3048 and 3149) exist in the wild-type PCR product, but the 3048 site is disrupted by the VP1 I192F WIN-R mutation (**Fig. 7c**). We brought PCR reactions to 200- μ l total volumes and digested them with 25 units of *TfiI* for 2 h at 65 °C. We then precipitated the reactions with ethanol and analyzed them by PAGE on a 5% polyacrylamide, 8 M urea gel.

Protein Data Bank accession number. Crystal structure of Mahoney strain of poliovirus at 2.2 Å resolution, 1HXS.

Note: Supplementary information is available on the Nature Genetics website.

ACKNOWLEDGMENTS

We thank S. Dutcher, P. Sarnow and J. Theriot for reading the manuscript; P. Harbury for editing; J.M. Lyle for experimental insights; and A. Mosser and A. Macadam for advice and reagents. This work was supported by the US National Institutes of Health (National Research Service Award to S.C.), the Hutchison Program in Translational Medicine and the Ellison Medical Foundation.

COMPETING INTERESTS STATEMENT

The authors declare that they have no competing financial interests.

Received 16 December 2004; accepted 14 April 2005

Published online at <http://www.nature.com/naturegenetics/>

- Domingo, E. & Holland, J.J. RNA virus mutations and fitness for survival. *Annu. Rev. Microbiol.* **51**, 151–178 (1997).
- Ledinko, N. & Hirst, G.K. Mixed infection of HeLa cells with polioviruses types 1 and 2. *Virology* **14**, 207–219 (1961).
- Holland, J.J. & Cords, C.E. Maturation of poliovirus RNA with capsid protein coded by heterologous enteroviruses. *Proc. Natl. Acad. Sci. USA* **51**, 1082–1085 (1964).
- Ikegami, N., Eggers, H.J. & Tamm, I. Rescue of drug-requiring and drug-inhibited enteroviruses. *Proc. Natl. Acad. Sci. USA* **52**, 1419–1426 (1964).
- Holland, J.J. *et al.* Virus mutation frequencies can be greatly underestimated by monoclonal antibody neutralization of virions. *J. Virol.* **63**, 5030–5036 (1989).
- Paul, A.V. Possible unifying mechanism of picornavirus genome replication. in *Molecular Biology of Picornaviruses* (eds. B.L. Semler & E. Wimmer) 227–246 (ASM Press, Washington, D.C., 2002).
- Kaplan, G. & Racaniello, V.R. Construction and characterization of poliovirus sub-genomic replicons. *J. Virol.* **62**, 1687–1696 (1988).
- Novak, J.E. & Kirkegaard, K. Coupling between genome translation and replication in an RNA virus. *Genes Dev.* **8**, 1726–1737 (1994).
- Lyle, J.M., Bullitt, E., Bienz, K. & Kirkegaard, K. Visualization and functional analysis of RNA-dependent RNA polymerase lattices. *Science* **296**, 2218–2222 (2002).
- Thompson, A.A. & Peersen, O.B. Structural basis for proteolysis-dependent activation of the poliovirus RNA-dependent RNA polymerase. *EMBO J.* **23**, 3462–3471 (2004).
- Paul, A.V., Rieder, E., Kim, D.W., van Boom, J.H. & Wimmer, E. Identification of an RNA hairpin in poliovirus RNA that serves as the primary template in the *in vitro* uridylylation of VPg. *J. Virol.* **74**, 10359–10370 (2000).
- Herskowitz, I. Functional inactivation of genes by dominant negative mutations. *Nature* **329**, 219–222 (1987).
- Yin, J., Paul, A.V., Wimmer, E. & Rieder, E. Functional dissection of a poliovirus cis-acting replication element [PV-cre(2C)]: analysis of single- and dual-cre viral genomes and proteins that bind specifically to PV-cre RNA. *J. Virol.* **77**, 5152–5166 (2003).
- Murray, K.E. & Barton, D.J. Poliovirus CRE-dependent VPg uridylylation is required for positive-strand RNA synthesis but not for negative-strand RNA synthesis. *J. Virol.* **77**, 4739–4750 (2003).
- Aldino, R., Rieckhof, G.E., Achacoso, P.L. & Baltimore, D. Poliovirus RNA synthesis utilizes an RNP complex formed around the 5'-end of viral RNA. *EMBO J.* **12**, 3587–3598 (1993).
- Hambidge, S.J. & Sarnow, P. Translational enhancement of the poliovirus 5' noncoding region mediated by virus-encoded polypeptide 2A. *Proc. Natl. Acad. Sci. USA* **89**, 10272–10276 (1992).
- Macadam, A.J. *et al.* 1994. Role for poliovirus protease 2A in cap independent translation. *EMBO J.* **13**, 924–927 (1994).
- Toyoda, H. *et al.* A second virus-encoded proteinase involved in proteolytic processing of poliovirus polyprotein. *Cell* **45**, 761–770 (1986).
- Hellen, C.U., Lee, C.K. & Wimmer, E. Determinants of substrate recognition by poliovirus 2A proteinase. *J. Virol.* **66**, 3330–3338 (1992).
- Lyons, T., Murray, K.E., Roberts, A.W. & Barton, D.J. Poliovirus 5'-terminal cloverleaf RNA is required in cis for VPg uridylylation and the initiation of negative-strand RNA synthesis. *J. Virol.* **75**, 10696–10708 (2001).
- Agut, H. *et al.* A point mutation in the poliovirus polymerase gene determines a complementable temperature-sensitive defect of RNA replication. *Virology* **168**, 302–311 (1989).
- Charini, W.A., Burns, C.C., Ehrenfeld, E. & Semler, B.L. *trans* rescue of a mutant poliovirus RNA polymerase function. *J. Virol.* **65**, 2655–2665 (1991).
- Johnson, K.L. & Sarnow, P. Three poliovirus 2B mutants exhibit noncomplementable defects in viral RNA amplification and display dosage-dependent dominance over wild-type poliovirus. *J. Virol.* **65**, 4341–4349 (1991).
- Compton, S.R., Nelsen, B. & Kirkegaard, K. Temperature-sensitive poliovirus mutant fails to cleave VPO and accumulates provirions. *J. Virol.* **64**, 4067–4075 (1990).
- Hope, D.A., Diamond, S.E. & Kirkegaard, K. Genetic dissection of interaction between poliovirus 3D polymerase and viral protein 3AB. *J. Virol.* **71**, 9490–9498 (1997).
- Fox, M.P., Otto, M.J. & McKinlay, M.A. Prevention of rhinovirus and poliovirus uncoating by WIN 51711, a new antiviral drug. *Antimicrob. Agents Chemother.* **30**, 110–116 (1986).

27. Chapman, M.S., Minor, I., Rossmann, M.G., Diana, G.D. & Andries, K. Human rhinovirus 14 complexed with antiviral compound R 61837. *J. Mol. Biol.* **217**, 455–463 (1991).
28. Mosser, A.G., Sgro, J.Y. & Rueckert, R.R. Distribution of drug resistance mutations in type 3 poliovirus identifies three regions involved in uncoating functions. *J. Virol.* **68**, 8193–8201 (1994).
29. Pevear, D.C., Tull, T.M., Seipel, M.E. & Groarke, J.M. Activity of pleconaril against enteroviruses. *Antimicrob. Agents Chemother.* **43**, 2109–2115 (1999).
30. Jubelt, B., Wilson, A.K., Ropka, S.L., Guidinger, P.L. & McKinlay, M.A. Clearance of a persistent human enterovirus infection of the mouse central nervous system by the antiviral agent disoxaril. *J. Infect. Dis.* **159**, 866–871 (1989).
31. Groarke, J.M. & Pevear, D.C. Attenuated virulence of pleconaril-resistant coxsackievirus B3 variants. *J. Infect. Dis.* **179**, 1538–1541 (1999).
32. Preugschat, F., Yao, C.-W. & Strauss, J.H. In vitro processing of Dengue virus type 2 nonstructural proteins NS2A, NS2B, and NS3. *J. Virol.* **64**, 4364–4374 (1990).
33. Rost, B. & Sander, C. Conservation and prediction of solvent accessibility in protein families. *Proteins* **20**, 216–226 (1994).
34. Ho, S.N., Hunt, H.D., Horton, R.M., Pullen, J.K. & Pease, L.R. Site-directed mutagenesis by overlap extension using the polymerase chain reaction. *Gene* **77**, 51–59 (1989).
35. Kirkegaard, K. Mutations in VP1 of poliovirus specifically affect both encapsidation and release of viral RNA. *J. Virol.* **64**, 195–206 (1990).
36. Barton, D.J., O'Donnell, B.J. & Flanagan, J.B. 5' cloverleaf in poliovirus RNA is a cis-acting replication element required for negative-strand synthesis. *EMBO J.* **20**, 1439–1448 (2001).
37. Jarvis, T.C. & Kirkegaard, K. Poliovirus RNA recombination: mechanistic studies in the absence of selection. *EMBO J.* **11**, 3135–3145 (1992).
38. Ansardi, D.C. & Morrow, C.D. Amino acid substitutions in the poliovirus maturation cleavage site affect assembly and result in accumulation of provirions. *J. Virol.* **69**, 1540–1547 (1995).
39. Reynolds, C., Page, G., Zhou, H. & Chow, M. Identification of residues in VP2 that contribute to poliovirus neutralization antigenic site 3B. *Virology* **184**, 391–396 (1991).
40. Yu, S.F. & Lloyd, R.E. Identification of essential amino acid residues in the functional activity of poliovirus 2A proteinase. *Virology* **182**, 615–625 (1991).
41. Rothberg, P.G., Harris, T.J., Nomoto, A. & Wimmer, E. O4-(5'-uridylyl)tyrosine is the bond between the genome-linked protein and the RNA of poliovirus. *Proc. Natl. Acad. Sci. USA* **75**, 4868–4872 (1978).
42. Ambros, V. & Baltimore, D. Protein is linked to the 5' end of poliovirus RNA by a phosphodiester linkage to tyrosine. *J. Biol. Chem.* **253**, 5263–5266 (1978).
43. Hammerle, T., Hellen, C.U. & Wimmer, E. Site-directed mutagenesis of the putative catalytic triad of poliovirus 3C proteinase. *J. Biol. Chem.* **266**, 5412–5416 (1991).
44. Hobson, S.D. *et al.* Oligomeric structures of poliovirus polymerase are important for function. *EMBO J.* **20**, 1153–1163 (2001).
45. Hansen, J.L., Long, A.M. & Schultz, S.C. Structure of the RNA-dependent RNA polymerase of poliovirus. *Structure* **5**, 1109–1122 (1997).
46. Burns, C.C., Lawson, M.A., Semler, B.L. & Ehrenfeld, E. Effects of mutations in poliovirus 3Dpol on RNA polymerase activity and on polyprotein cleavage. *J. Virol.* **63**, 4866–4874 (1989).
47. Goodfellow, I. *et al.* Identification of a cis-acting replication element within the poliovirus coding region. *J. Virol.* **74**, 4590–4600 (2000).
48. Petersen, J.F. *et al.* The structure of the 2A proteinase from a common cold virus: a proteinase responsible for the shut-off of host-cell protein synthesis. *EMBO J.* **18**, 5463–5475 (1999).